

# A Molecular Peptide Beacon for the Ratiometric Sensing of Nucleic Acids

Junchen Wu,<sup>†,§</sup> Ying Zou,<sup>||</sup> Chunyan Li,<sup>||</sup> Wilhelm Sicking,<sup>†</sup> Ivo Piantanida,<sup>‡</sup> Tao Yi,<sup>\*,||</sup> and Carsten Schmuck<sup>\*,†</sup>

<sup>†</sup>Institute for Organic Chemistry, University of Duisburg-Essen, 45117 Essen, Germany

<sup>‡</sup>Ruder Bošković Institute, HR-10000 Zagreb, Croatia

<sup>§</sup>Key Laboratory for Advanced Materials and Institute of Fine Chemicals, East China University of Science and Technology, Shanghai 200237, China

<sup>||</sup>Department of Chemistry, Fudan University, Shanghai 200438, China

**S** Supporting Information

**ABSTRACT:** A pyrene-functionalized cationic oligopeptide **1** efficiently binds to double-stranded DNA, as shown by different spectrophotometric studies. Upon binding, the conformation of **1** changes from a folded to an extended form, which leads to a distinct change in the fluorescence properties. Thus, **1** functions as a molecular peptide beacon, and as it is easily taken up by cells, **1** can also be used for imaging of nucleic acids within cells.

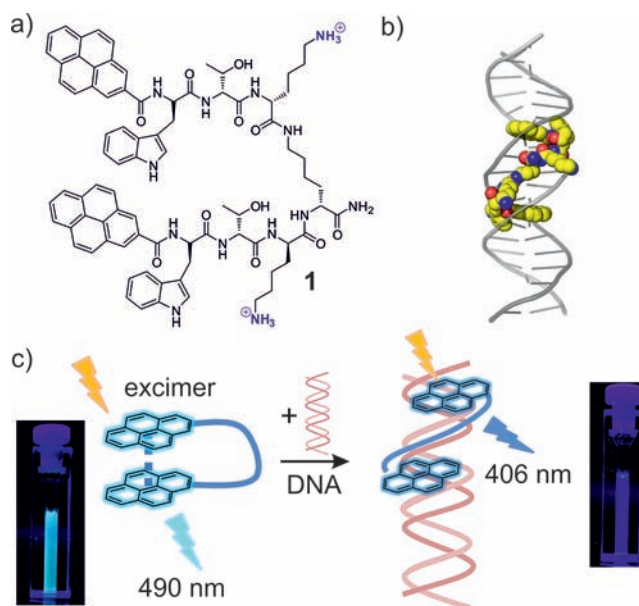
The sensing of nucleic acids is of particular interest for biomedical research. In this context, molecular beacons (MBs) are often used,<sup>1</sup> in which a synthetic oligonucleotide is functionalized with two chromophores, most often at its ends. Hybridization with a complementary DNA strand induces a conformational change of the probe that changes the interaction of the two chromophores, giving rise to a specific spectroscopic signal that is used for detection. Some recent developments in this area include pyrene-functionalized oligonucleotides and locked nucleic acid (LNAs),<sup>2</sup> quencher-free MBs,<sup>3</sup> wavelength-shifting MBs,<sup>4</sup> and MBs based on excimer fluorescence color readout.<sup>5</sup> Besides pure oligonucleotide-based MBs, ones based on peptide nucleic acids (PNAs) have also been reported.<sup>6</sup> However, the use of such MBs for imaging of nucleic acids in cells requires the additional use of artificial transfection vectors, as these MBs are not able to enter cells directly.<sup>1</sup> MBs derived from oligopeptides, called peptide beacons (PBs),<sup>7</sup> have been much less explored, as small oligopeptides often do not form stable self-assembled “closed” structures that can then undergo a spectroscopically detectable conformational change upon binding to an analyte. Only few examples of PBs have thus been reported, mainly used to date for protein sensing.<sup>8</sup> As small cationic peptides can both bind to nucleic acids and also sometimes penetrate cells,<sup>9</sup> the use of PBs for imaging of nucleic acids within cells is attractive.

We present here a pyrene-based PB, **1**, that efficiently interacts with double-stranded DNA (ds-DNA), as shown by spectrophotometric studies *in vitro*. Upon binding, **1** shows a distinct fluorescence change from the emission of a pyrene excimer in free **1** to a monomer emission in the complex with the nucleic acid. This change in fluorescence depends on the sequence of the

nucleic acid, allowing for ratiometric sensing of AT-rich versus GC-rich sequences. Furthermore, PB **1** is efficiently taken up by cells, enabling the imaging of nucleic acids in cells using fluorescence microscopy without the need for any additional transfection vectors to facilitate cell uptake.

Our group has long-standing expertise in the development of artificial receptors and sensors for anionic biomolecules such as peptides and proteins,<sup>10</sup> nucleotides and nucleic acids,<sup>11</sup> and even bacterial cell wall components.<sup>12</sup> Our idea was now to use an artificial DNA-binding peptide as a sensor for imaging of nucleic acids in cells. For this purpose, the molecular PB **1** was designed (Scheme 1). **1** contains two Trp-Thr-Lys tripeptide units,

**Scheme 1.** (a) Molecular Structure of **1**; (b) Possible Binding Mode of **1** Bound to p(dA·dT)<sub>2</sub> According to Molecular Modeling; (c) Cartoon Representation of Peptide Beacon **1** and Its Interaction with Nucleic Acid (the Photographs Show the Corresponding Cuvettes under UV Light)



Received: November 4, 2011

Published: January 13, 2012

each attached via its C-terminus to a central lysine spacer. At its N-terminus, each peptide arm is functionalized with a pyrene moiety. Pyrene is often used as a polarity-sensitive probe for polynucleotide sensing because it can not only intercalate into ds-DNA but also bind to the grooves. In each case, specific changes in its fluorescence properties are observed.<sup>2</sup> The amino acids used were expected to enable binding to the anionic nucleic acids and also render the overall molecule sufficiently polar for applications in water. Molecular PB **1** was synthesized using microwave-assisted solid-phase peptide synthesis [for details, see the Supporting Information (SI)].

The emission spectrum of **1** features a strong band at  $\lambda = 490$  nm and a significantly weaker one at 406 nm (Figure 1a).

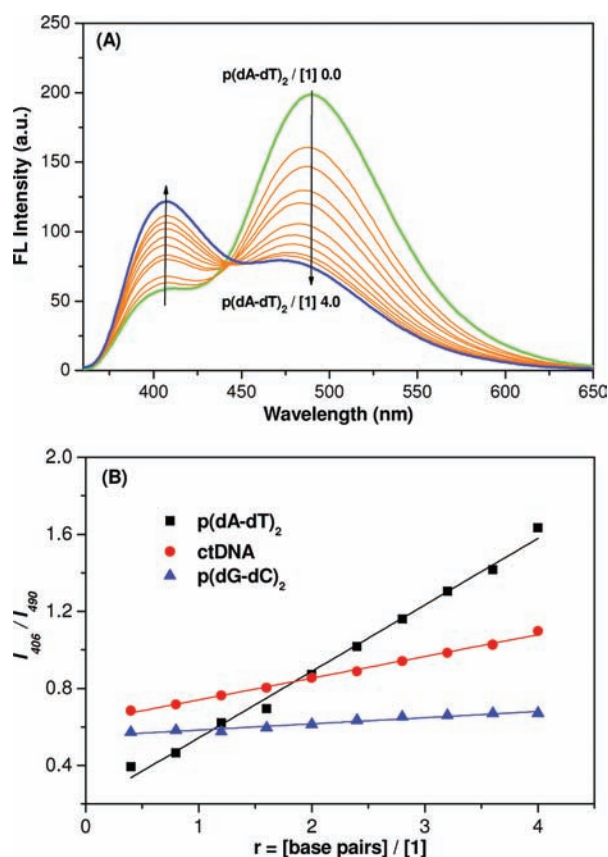


**Figure 1.** (A) Fluorescence emission spectra for the titration of a 10  $\mu\text{M}$  solution of **1** with  $\text{p}(\text{dA}\cdot\text{dT})_2$  at 25  $^\circ\text{C}$  in aqueous buffer (pH 7.4) (with base pair/**1** molar ratios ranging from 0 to 4.0). (B) Ratiometric calibration curves for  $I_{406}/I_{490}$  as functions of the base pair/**1** molar ratio for different base pairs ( $\lambda_{\text{ex}} = 340$  nm). The different starting values are due to the use of different cuvettes in the experiments.

The band at 406 nm arises from a single pyrene chromophore whereas the band at 490 is typical for a pyrene excimer, indicating that the two pyrene units in **1** are mostly  $\pi$ -stacked in free solution. Hence, **1** adopts an intramolecularly folded structure, as required for an MB. Upon binding to ds-DNA, this excimer emission decreases, and the monomer emission increases accordingly (Figure 1a). Finally the excimer emission completely disappears, and only the monomer emission remains (Figure S1 in the SI). Obviously, **1** binds to the polynucleotide in such a way that the molecule unfolds and the pyrene excimer can no longer form. These spectroscopic changes depend on the type of polynucleotide and are most pronounced for  $\text{p}(\text{dA}\cdot\text{dT})_2$  and

less for  $\text{p}(\text{dG}\cdot\text{dC})_2$  and calf-thymus DNA (ctDNA) having ca. 60% AT and 40% GC (Figures S1 and S2). Interestingly, the relative intensities of the two emission bands at 406 and 490 nm can be used for ratiometric detection<sup>13</sup> of  $\text{p}(\text{dA}\cdot\text{dT})_2$  relative to other nucleic acids, as the ratio of the fluorescence intensities ( $I_{406}/I_{490}$ ) is much larger for  $\text{p}(\text{dA}\cdot\text{dT})_2$  than for ctDNA or  $\text{p}(\text{dG}\cdot\text{dC})_2$  (Figure 1B).

The DNA-binding properties of **1** were further characterized by circular dichroism (CD) studies. PB **1** exhibits a distinct CD spectrum of its own with two positive bands at ca. 253 and 372 nm and three negative bands at ca. 225, 286, and 338 nm (Figure 2A) corresponding to the absorption maxima of the

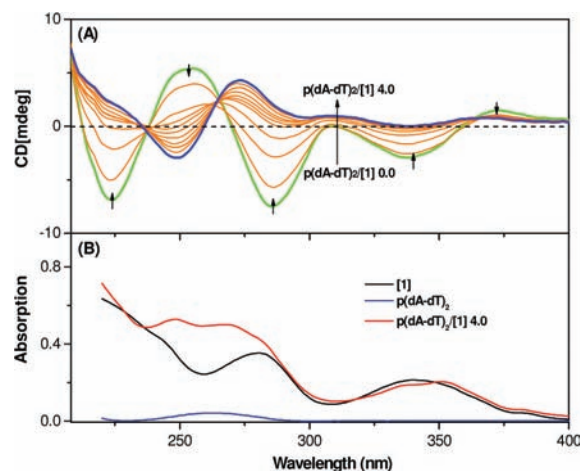


**Figure 2.** (A) CD titration of a 10  $\mu\text{M}$  solution of **1** with  $\text{p}(\text{dA}\cdot\text{dT})_2$  in aqueous bis-Tris-HCl buffer (TBS) at pH 7.4. (B) Absorption spectra of 10  $\mu\text{M}$  solutions of **1**,  $\text{p}(\text{dA}\cdot\text{dT})_2$ , and  $1/\text{p}(\text{dA}\cdot\text{dT})_2$  (base pair/**1** molar ratio = 4.0) in TBS buffer (pH 7.4) at 25  $^\circ\text{C}$ .

pyrene moieties. The two bisignate CD bands (a strong one at 253/286 nm and weaker one at 338/372 nm) also indicate a folded  $\pi$ -stacked structure of the two pyrene moieties in free **1**, as already evidenced by the strong excimer emission in the fluorescence spectrum. Upon addition of  $\text{p}(\text{dA}\cdot\text{dT})_2$ , the CD bands of **1** decrease and finally completely disappear, resulting in the pure CD spectrum of  $\text{p}(\text{dA}\cdot\text{dT})_2$  (Figure 2A and Figure S3C). Similar observations were made with ctDNA and  $\text{p}(\text{dG}\cdot\text{dC})_2$  (Figure S3).

Processing of the fluorimetric and CD titration data using the Scatchard equation<sup>14</sup> indicates that the affinity of **1** for the nucleic acids is in the micromolar range (for details see Figure S4), again with a clear preference for  $\text{p}(\text{dA}\cdot\text{dT})_2$  ( $K_s = 20$   $\mu\text{M}$ ) over  $\text{p}(\text{dG}\cdot\text{dC})_2$  ( $K_s = 300$   $\mu\text{M}$ ). In addition, the ratio  $n_{[\text{DNA}]/[\text{1}]}$  also changes accordingly as  $n(\text{AT}) > n(\text{ctDNA}) > n(\text{GC})$ , which shows that the density of binding sites per base pair decreases with decreasing number of AT base pairs. This preference of **1** for AT-rich sequences hints at the involvement of the minor groove for binding of **1** (see below). These data confirm that **1** has a high affinity for ds-DNA and can be used as a molecular PB for the sensing of nucleic acids (Scheme 1c). Molecular modeling calculations (Schrödinger version 9.8, OPLS force field, water solvation model) suggest that **1** can bind in an extended conformation into the minor groove of  $\text{p}(\text{dA}\cdot\text{dT})_2$  (see Scheme 1B). In the calculated binding mode, the two pyrenes intercalate into the base stack, whereas the peptide linker is aligned along the minor groove of the nucleic acid,

with additional electrostatic interactions between the positively charged lysine side chains and the phosphate backbone. This is in line with the behavior of most other small DNA-binding molecules, which also bind into the minor groove of ds-DNA.<sup>15</sup> Such a binding mode also explains the observed changes in the fluorescence of **1**. Upon complexation, **1** has to unfold, and accordingly, the pyrene excimer fluorescence disappears while the monomer emission from the bound state increases (Figure 1 and Figure S1E). A 4',6-diamidino-2-phenylindole (DAPI) displacement assay confirmed minor-groove binding as a reasonable binding mode. DAPI exclusively binds in the minor groove of AT sequences of ds-DNA<sup>16</sup> but is efficiently displaced by the addition of **1** (Figure S5), indicating that **1** can compete with DAPI for binding in the minor groove. Minor-groove binding also explains the observed preference of **1** for AT-rich DNA sequences. For example, p(dA·dT)<sub>2</sub> has a well-defined, appropriately spaced, and easily accessible minor groove. However, p(dG·dC)<sub>2</sub> has a minor groove that is ca. 2 Å narrower than that of p(dA·dT)<sub>2</sub> and significantly less well suited for binding of other molecules because of steric hindrance by the protruding amino group of guanine.

DNA imaging in live cells was evaluated with HeLa cell lines using confocal laser scanning microscopy (CLSM). Fluorescent images of individual fixed cells treated with **1** clearly showed that **1** is capable of entering the cell, reaching the nucleus, and binding to the nucleic acids there, giving rise to a strong fluorescence signal coming from the nucleus (Figure 3). Quantification

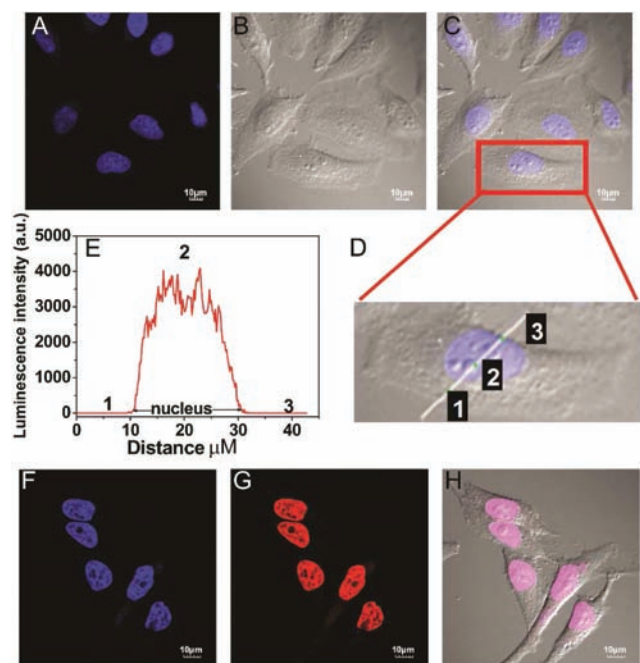


**Figure 3.** (A–C) CLSM images of HeLa cells incubated with **1** in physiological saline (10 μM) for 30 min at 37 °C. (B) and (C) are bright-field and overlay images of (A), respectively. (D) Amplified imaging of one cell [red square in (C)]. (E) Cross-sectional analysis (along the white line in image D) indicated that the luminescence stems exclusively from the nucleus (spot 2) and not from the cytoplasm (spot 3). (F–H) CLSM images of (F) HeLa cells incubated for 30 min at 37 °C with **1** in physiological saline (10 μM) and (G) HeLa cells fixed by MeOH and then stained with PI containing RNAase; (H) is the overlay image of (F), (G), and the corresponding bright-field image (I:  $\lambda_{\text{ex}} = 405 \text{ nm}$ ,  $\lambda_{\text{em}} = 425 \pm 10 \text{ nm}$ ; PI:  $\lambda_{\text{ex}} = 488 \text{ nm}$ ,  $\lambda_{\text{em}} = 620 \pm 10 \text{ nm}$ ).

of the luminescence intensity plot revealed an extraordinarily high signal-to-background ratio between the nucleus (>1000) and the cytoplasm (Figure 3E), indicating exclusive staining of the cell nucleus. Practically no fluorescence was observed from the cytoplasm. Colocalization studies with propidium iodide (PI), a dye that specifically localizes in the nucleus, confirmed these findings that **1** was found only in the nucleus of the cell (Figure 3). Further exploration of **1** for staining of nucleic acids within the nucleus of the cell was carried out by serially scanning at increasing depths along the *z* axis. The nucleus region of the cells were clearly visualized in the serial *xz* cross-sectional images (Figure 3E; also see Figures S6 and S7), again indicating that the luminescence enhancement occurred exclusively in the nucleus. Cell uptake of **1** showed a pronounced temperature effect. At 4 °C, HeLa cells could not uptake **1**, and no DNA staining occurred (Figure S8). At 37 °C, however, uptake of **1** into the cells and subsequent staining of nuclear DNA was observed (Figure 3 and Figure S8D), suggesting that cell uptake of **1** occurs in an energy-dependent fashion, most likely via endocytosis.<sup>17</sup>

For potential applications, the cell toxicity of **1** toward the HeLa cell line was measured using a standard MTT assay and flow cytometry (statistical analysis) (Figure 4 and Figure S9).

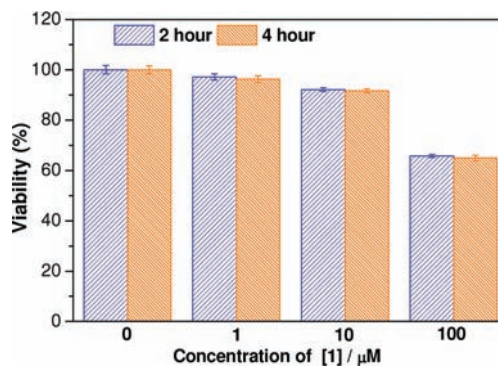


**Figure 4.** Cell viability values (%) estimated by MTT proliferation test at different concentrations of **1**. HeLa cells were cultured in the presence of **1** at 37 °C for 2 or 4 h.

At a **1** concentration of 10.0 μM, cell viabilities were estimated to be greater than 92% and 91% after incubation for 2 and 4 h, respectively. Even at a significantly higher concentration of 100 μM, cell viabilities were still nearly 70%. For a statistical analysis, we performed flow cytometry measurements, which also confirmed cell viabilities of over 97% at a concentration of 10 μM (Table S1 in the SI). Hence, **1** has no general cytotoxicity.

In conclusion, we have demonstrated that the pyrene-functionalized oligopeptide **1** can be used as a molecular peptide beacon to sense ds-DNA. Upon binding to nucleic acids, **1** undergoes a conformational change from a folded to an extended form that switches the fluorescence of **1** from an excimer emission to a monomer emission. PB **1** can thus be used for the ratiometric sensing of different types of polynucleotides, as binding to p(dA·dT)<sub>2</sub> is preferred to GC-containing polynucleotides. Furthermore, PB **1** is taken up by cells and can thus be used for the staining of nuclear DNA using fluorescence microscopy. As **1** does not possess any general cytotoxicity, it might be of interest for applications in diagnostics. We are currently working on increasing the sensitivity of the system by testing chromophores other than pyrene.

**■ ASSOCIATED CONTENT****■ Supporting Information**

Details of syntheses; characterization data; and UV–vis, fluorescence, CD, and NMR spectra. This material is available free of charge via the Internet at <http://pubs.acs.org>.

**■ AUTHOR INFORMATION****Corresponding Author**

yitao@fudan.edu.cn; carsten.schmuck@uni-due.de

**■ ACKNOWLEDGMENTS**

J.W. thanks the Alexander von Humboldt Foundation for a postdoctoral fellowship. We thank Christine Kallweit (Institute of Organic Chemistry, University of Duisburg-Essen, Germany) for measuring the CD spectra. T.Y. thanks the National Science Foundation of China (NSFC) for support (30890141 and 21125104).

**■ REFERENCES**

- (1) Wang, K.; Tang, Z.; Chaoyong, J. Y.; Kim, Y.; Fang, X.; Li, W.; Wu, Y.; Medley, C. D.; Cao, Z.; Li, J.; Colon, P.; Lin, H.; Tan, W. *Angew. Chem., Int. Ed.* **2009**, *48*, 856–870.
- (2) Østergaard, M. E.; Hrdlicka, P. J. *Chem. Soc. Rev.* **2011**, *40*, 5771–5788.
- (3) (a) Hwang, G. T.; Seo, Y. J.; Kim, H. B. *J. Am. Chem. Soc.* **2004**, *126*, 6528–6529. (b) Venkatesan, N.; Seo, Y. J.; Kim, H. B. *Chem. Soc. Rev.* **2008**, *37*, 648–663.
- (4) (a) Socher, E.; Jarikote, D. V.; Knoll, A.; Röglin, L.; Burmeister, J.; Seitz, O. *Anal. Biochem.* **2008**, *375*, 318–330. (b) Socher, E.; Berthge, L.; Knoll, A.; Jungnick, N.; Herrmann, A.; Seitz, O. *Angew. Chem., Int. Ed.* **2008**, *47*, 9555–9559.
- (5) (a) Berndt, S.; Wagenknecht, H.-A. *Angew. Chem., Int. Ed.* **2009**, *48*, 2418–2421. (b) Häner, R.; Biner, S. M.; Langenegger, S. M.; Meng, T.; Malinovsky, V. L. *Angew. Chem., Int. Ed.* **2010**, *49*, 1227–1230. (c) Hara, Y.; Fujii, T.; Kashida, H.; Sekiguchi, K.; Liang, X.; Niwa, K.; Takase, T.; Yoshida, Y.; Asanuma, H. *Angew. Chem., Int. Ed.* **2010**, *49*, 5502–5506. (d) Kashida, H.; Takatsu, T.; Fujii, T.; Sekiguchi, K.; Liang, X.; Niwa, K.; Takase, T.; Yoshida, Y.; Asanuma, H. *Angew. Chem., Int. Ed.* **2009**, *48*, 7044–7047. (e) Holzhauser, C.; Wagenknecht, H. A. *Angew. Chem., Int. Ed.* **2011**, *50*, 7268–7272.
- (6) (a) Kummer, S.; Knoll, A.; Socher, E.; Bethge, L.; Herrmann, A.; Seitz, O. *Angew. Chem., Int. Ed.* **2011**, *50*, 1931–1934. (b) Vasilyeva, E.; Lam, B.; Fang, Z.; Minden, M. D.; Sargent, E. H.; Kelley, S. O. *Angew. Chem., Int. Ed.* **2011**, *50*, 4137–4141.
- (7) (a) Oh, K. J.; Cash, K. J.; Plaxco, K. W. *Chem.—Eur. J.* **2009**, *15*, 2244–2251. (b) Pazos, E.; Vazquez, L.; Mascarenas, J. L.; Vazquez, M. E. *Chem. Soc. Rev.* **2009**, *38*, 3348–3359.
- (8) (a) Oh, K. J.; Cash, K. J.; Plaxco, K. W. *J. Am. Chem. Soc.* **2006**, *128*, 14018–14019. (b) Oh, K. J.; Cash, K. J.; Hugenberg, V.; Plaxco, K. W. *Bioconjugate Chem.* **2007**, *18*, 607–609.
- (9) (a) Hassane, F. S.; Saleh, A. F.; Abes, R.; Gait, M. J.; Lebleu, B. *Cell. Mol. Life Sci.* **2010**, *67*, 715–726. (b) Pujals, S.; Giralt, E. *Adv. Drug Delivery Rev.* **2008**, *60*, 473–484. (c) Stewart, K. M.; Horton, K. L.; Kelley, S. O. *Org. Biomol. Chem.* **2008**, *6*, 2242–2255.
- (10) (a) Schmuck, C.; Geiger, L. *J. Am. Chem. Soc.* **2004**, *126*, 8898–8899. (b) Schmuck, C.; Wich, P. *Angew. Chem., Int. Ed.* **2006**, *45*, 4277–4281. (c) Wich, P. R.; Schmuck, C. *Angew. Chem., Int. Ed.* **2010**, *49*, 4113–4116.
- (11) Kuchelmeister, H. Y.; Schmuck, C. *Chem.—Eur. J.* **2011**, *17*, 5311–5318.
- (12) Wu, J.; Zawistowski, A.; Ehrmann, M.; Yi, T.; Schmuck, C. *J. Am. Chem. Soc.* **2011**, *133*, 9720–9723.
- (13) Xu, Z.; Singh, N. J.; Lim, J.; Pan, J.; Kim, H. N.; Park, S.; Kim, K. S.; Yoon, J. *J. Am. Chem. Soc.* **2009**, *131*, 15528–15533.
- (14) McGhee, J. D.; von Hippel, P. H. *J. Mol. Biol.* **1974**, *86*, 469–489.
- (15) Liu, Y.; Kumar, A.; Depauw, S.; Nhili, R.; Cordonnier, M. H. D.; Lee, M. P.; Ismail, M. A.; Farahat, A. A.; Say, M.; Catoen, S. C.; Parra, A. B.; Needle, S.; Boykin, D. W.; Wilson, W. D. *J. Am. Chem. Soc.* **2011**, *133*, 10171–10183.
- (16) Tanius, F. A.; Veal, J. M.; Buczak, H.; Ratmeyer, L. S.; Wilson, W. D. *Biochemistry* **1992**, *31*, 3103–3112.
- (17) Sinfreu, J. F.; Giralt, E.; Castel, S.; Albericio, F.; Royo, M. *J. Am. Chem. Soc.* **2005**, *127*, 9459–9468.